This article was downloaded by:
On: *25 January 2011*
Access details: *Access Details: Free Access*
Publisher *Taylor & Francis*
Informa Ltd Registered in England and Wales Registered Number: 1072954 Registered office: Mortimer House, 37-41 Mortimer Street, London W1T 3JH, UK

Separation Science and Technology
Publication details, including instructions for authors and subscription information:
http://www.informaworld.com/smpp/title~content=t713708471

CFD Study on the Effect of Hydrocyclone Structure on the Separation Efficiency of Fine Particles

Kuo-Jen Hwang[a]; Wen-Hao Wu[a]; Shaoxiang Qian*[a]; Youichi Nagase†[a]
[a] Department of Chemical and Materials Engineering, Tamkang University, Tamsui, Taipei Hsien, Taiwan

To cite this Article Hwang, Kuo-Jen , Wu, Wen-Hao , Qian*, Shaoxiang and Nagase†, Youichi(2008) 'CFD Study on the Effect of Hydrocyclone Structure on the Separation Efficiency of Fine Particles', Separation Science and Technology, 43: 15, 3777 — 3797
To link to this Article: DOI: 10.1080/01496390802286637
URL: http://dx.doi.org/10.1080/01496390802286637

PLEASE SCROLL DOWN FOR ARTICLE

Full terms and conditions of use: http://www.informaworld.com/terms-and-conditions-of-access.pdf

This article may be used for research, teaching and private study purposes. Any substantial or systematic reproduction, re-distribution, re-selling, loan or sub-licensing, systematic supply or distribution in any form to anyone is expressly forbidden.

The publisher does not give any warranty express or implied or make any representation that the contents will be complete or accurate or up to date. The accuracy of any instructions, formulae and drug doses should be independently verified with primary sources. The publisher shall not be liable for any loss, actions, claims, proceedings, demand or costs or damages whatsoever or howsoever caused arising directly or indirectly in connection with or arising out of the use of this material.

Separation Science and Technology, 15: 3777–3797, 2008
Copyright © Taylor & Francis Group, LLC
ISSN: 0149-6395 print/1520-5754 online
DOI: 10.1080/01496390802286637

Taylor & Francis
Taylor & Francis Group

CFD Study on the Effect of Hydrocyclone Structure on the Separation Efficiency of Fine Particles

Kuo-Jen Hwang[1], Wen-Hao Wu[1], Shaoxiang Qian,[1]* and Youichi Nagase[1]†
[1]Department of Chemical and Materials Engineering, Tamkang University, Tamsui, Taipei Hsien, Taiwan

Downloaded At: 09:08 25 January 2011

Abstract: Effects of geometric structure parameters of 10 mm-diameter hydrocyclones on the particle separation efficiency are studied using computational fluid dynamics (CFD). The fluid velocity profiles and particle trajectories are simulated using *RFLOW* software with a standard isotropic k-ε turbulent model. The JIS standard $CaCO_3$-17 particles are adopted as a particulate sample in simulations and experiments. Comparing the simulated results with experimental data, a maximum deviation about 20% in partition curves occurs for 5–10 μm particles. However, fairly good agreements for the cut-size predictions and the fish-hook phenomenon are obtained. The simulated cut-size d_{50} is only 2 μm larger than that measured in experiments, while the value of d_{100} can be accurately predicted. An increase in overflow diameter or a decrease in underflow diameter leads to a lower separation efficiency but a clearer separation sharpness due to lower fluid underflow rate. A short-and-wide rectangular inlet is more efficient for particle separation than a tall-and-narrow one. An inclined inlet conduit plays an inessential role on the efficiency improvement but gains a 2 μm reduction in d_{100}. Comparing the simulated results, the hydrocyclone used in the experiments of this study exhibits a higher separation

*Present address: Division of Technical Development, Advance Soft Corp., Tokyo 153-8904, Japan.
†Emeritus Professor of Department of Chemical Engineering, Hiroshima University, Japan.
Received 28 March 2008; accepted 19 May 2008.
Address correspondence to Kuo-Jen Hwang, Department of Chemical and Materials Engineering, Tamkang University, Tamsui, Taipei Hsien 25137, Taiwan. Fax: +886-2-26209887. E-mail: kjhwang@mail.tku.edu.tw

sharpness than the Rietema type and a higher efficiency than the Bradley type based on the same operation capacity and hydrocyclone size.

Keywords: CFD, hydrocyclone, particle classification, separation efficiency

INTRODUCTION

Hydrocyclone has been increasingly used in mineral, food, and chemical processes in recent years due to its low cost, high capacity, and simple operation. When particles are fed into a hydrocyclone tangentially, they will migrate rotationally and downward in the primary vortex. If the centrifugal and inertial forces are large enough, those particles will be collected into the underflow conduit. Otherwise, those small or light particles will be carried by the secondary vortex flowing out through the overflow conduit. Therefore, the centrifugal force produced in a hydrocyclone and the flow splits are the key factors to affect the particle separation efficiency. Since the size and geometric structure of a hydrocyclone have direct influences on these factors, to study how the geometric parameters affect the operation performance is the essential step for highly efficient hydrocyclone design.

Downloaded At: 09:08 25 January 2011

Computational Fluid Dynamics (CFD) is a useful method to simulate the fluid flow in various flow modules. Since it has many advantages, such as highly effective, economic, flexible, and time-saving for new apparatus design or process development, CFD has been employed in the hydrocyclone researches in the last decade. He et al. (1) developed a numerical method to simulate the 3-D flow and particle separation efficiency in a 76-mm Dabir's hydrocyclone. They employed cylindrical curvilinear grids and a modified k-ε turbulence model in CFD and predicted reasonably accurate fluid velocity profiles and particle separation curve. Cullivan et al. (2,3) used *FLUENT* software with an incorporation of a second-order pressure-strain Reynolds-stress turbulent model to simulate the profiles of fluid velocity, pressure and particle trajectories in hydrocyclones. A static asymmetric air-core was also simulated successfully. Schuetz et al. (4) modeled and simulated the flow pattern and separation efficiency in a 50-mm hydrocyclone using *FLUENT* software. An agreement between the simulated results and experimental data was obtained, and the possibilities and difficulties occurring in CFD methods were also reviewed. Grady et al. (5) used the computational fluid dynamics to predict the separation efficiency of oil drop in a 10 mm-diameter hydrocyclone. The deviations between the simulated results and experimental data for a given drop size were less than 20%. Olson and Van Ommen (6) have used the Reynolds stress turbulent model in CFD to simulate accurate velocity profiles in 250-mm hydrocyclones. Their simulated

particle recoveries for different vortex finder sizes agreed qualitatively with available experimental data. However, the feed solid concentration was indeed a notable limitation in the use of CFD. Narasimha et al. (7) used CFD modeling to predict the cut-size of particles under various conditions. The fluid flow was modeled by Navier-Stokes equations supplemented by a standard k-ε turbulence model using the *FLUENT* 6 package. The predicted water splits in the outlets and the cut-size for pure sand particles were reasonably in agreement with the experimental data measured in 101 mm-diameter hydrocyclones at low solid concentrations. Wang and Yu (8) studied the multiphase flow in hydrocyclones with different dimensions (lengths of cylindrical and conical parts and cyclone size) using CFD. They used the Reynolds stress model for multiphase turbulent flow, used the volume of multiphase model for the interface between liquid and air-core, and used the stochastic Lagrangian model for particle simulations. Their results indicated that the cylindrical section played an inessential role in the particle collection. Reducing the hydrocyclone size or increasing the length of conical section could improve the hydrocyclone performance. Recently, Bhaskar et al. (9) simulated the fluid flow in a 76 mm-diameter hydrocyclone using *FLUENT* software without air core and found that the use of the RSM turbulent model was better in agreement with the experimental of the water throughput than the standard k-ε or k-ε RNG models.

In practice, the cut-size and separation efficiency of particles are significantly determined by the hydrocyclone size. The smaller the cyclone is, the smaller the cut-size and the higher the efficiency will be. In recent years, small hydrocyclones with a diameter of 10-mm were developed and used for separating or classifying fine particles (10–12). However, a fish-hook phenomenon frequently occurred on the partition curve, which decreased the separation sharpness especially for submicron particles (11,12). Therefore, to enhance the separation efficiency and sharpness become the important criteria for new hydrocyclone design. In this study, the fluid flow and particle trajectory in 10-mm hydrocyclones are simulated using CFD. The effects of geometric structure parameters on the separation efficiency are studied and discussed. The performances of typical hydrocyclones are compared based on the same operation capacity and hydrocyclone size.

NUMERICAL METHODS

System and Meshes

A hydrocyclone with an inner-diameter of 10 mm in the cylindrical part and a length of 88 mm is analyzed in this study. The detail dimensions

Downloaded At: 09:08 25 January 2011

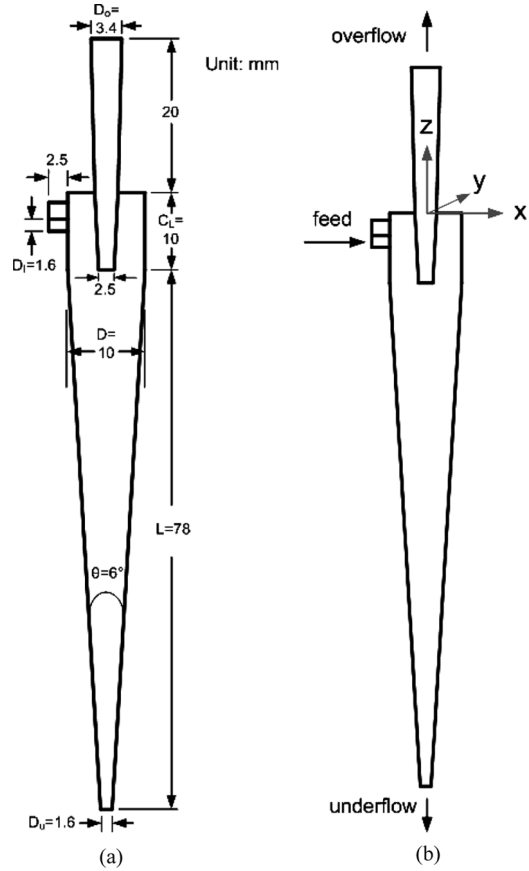

Figure 1. The hydrocyclone, (a) detail dimensions; (b) the system and coordinates.

and coordinate axes are shown in Figs. 1(a) and (b), respectively. The meshes and grids for numerical simulation are created by the *RFLOW* commercial software designed by *RFLOW* Co. in Tokyo, Japan. The Cartesian coordinate system is used in the mesh creation and numerical simulations. Drawing of the body geometry and 3-D meshes within the body should be carried out simultaneously. The main body of a hydrocyclone is divided into two sub-parts, cone and spiral parts, for mesh creation. The orthogonality of grid lines, the aspect ratio, and the connectivity of the grids are auto-checked by the software during the mesh creation. Figure 2 shows the typical results of mesh creation for the hydrocyclone using *RFLOW* software. The top view is shown in Fig. 2(a), while an overview can be seen in Fig. 2(b). The meshes become

Downloaded At: 09:08 25 January 2011

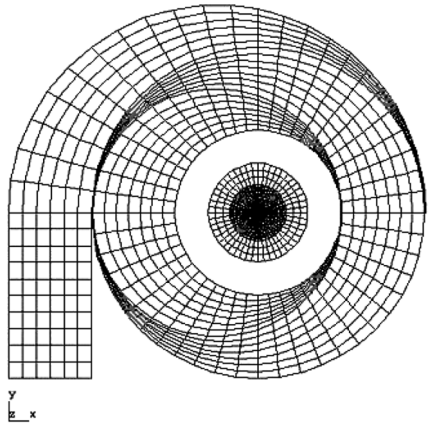

(a)

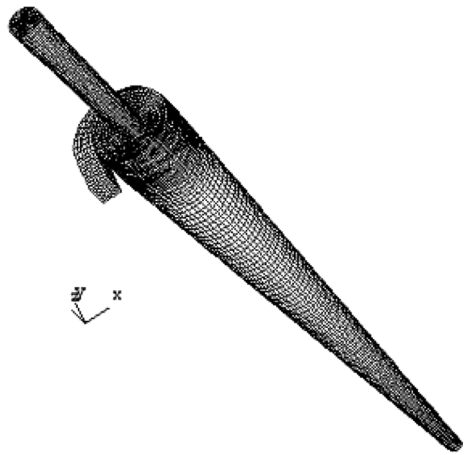

(b)

Figure 2. Finite volume mesh hydrocyclone geometry, (a) top view; (b) overview.

volute shapes following the entrance region because of the cylindrical wall and a slightly inclined inlet channel. In fact, the meshes in the system are not uniform; denser grid lines are established in the regions where exist higher velocity or pressure gradients.

Simulation of Fluid Flow

The governing equations used in the numerical simulation of fluid flow are summarized as follows.

Downloaded At: 09:08 25 January 2011

Continuity equation

$$\frac{\partial \rho}{\partial t} + (v \cdot \nabla)\rho + \rho \nabla \cdot v = 0 \tag{1}$$

where ρ is the fluid density, t is time, while v is the velocity vector.

Equations of motion

$$\rho\left(\frac{\partial v}{\partial t} + (v \cdot \nabla)v\right) = -\nabla p + \nabla((\mu + \mu_e)\nabla v) + \rho g \tag{2}$$

where p is the pressure and μ and μ_e are the fluid and eddy viscosities, respectively.

Downloaded At: 09:08 25 January 2011

A steady-state assumption is made in the simulation of fluid flow. The boundary conditions include:

(a) The density and viscosity of fluid are set to be $10^3\,\mathrm{kg/m^3}$ and 10^{-3} Pa.s, respectively.
(b) Non-slip conditions are set on the solid wall of hydrocyclone.
(c) A uniform velocity profile is set on the cross-section of feed inlet.
(d) The pressures at underflow and overflow outlets are set as constants. Since the split ratio of underflow to overflow rate is dependent on the pressure difference between the underflow and overflow outlets, the split ratio is fixed in simulation by adjusting the pressure difference between the underflow and overflow outlets.

The profiles of fluid velocity and pressure in the hydrocyclone are then simulated using *RFLOW* software. The standard k-ε isotropic turbulence model is employed for modeling the turbulence in the system. The convergence criteria are the residual of numerical computations being below 2.0×10^{-3} in fluid velocity evaluation and the ratio of the inflow rate to the overall outflow rate being 1.0 (mass balance).

Simulation of Particle Trajectory

The particle trajectories in the hydrocyclone are simulated using *RFLOW* software once the fluid velocity profiles are analyzed. The system is set at unsteady-state in the simulation. The physical properties of JIS $CaCO_3$-17 particles are used as the known conditions. The particle diameter

ranges from 0.26 to 22.60 μm, and the density is 2700 kg/m^3. The particle shape is assumed as spherical. The cross-section of the entrance is uniformly divided into 10×10 grids for setting the initial position of particles. A thin suspension is assumed; therefore, the interactions between particles are reasonably neglected. After setting the particle diameter and the inlet position, the particle trajectory is simulated by introducing the results of fluid flow analysis. The partial separation efficiency for the particles with a diameter of d, $\eta(d)$, can be considered as the mass fraction which can be collected into the underflow. As soon as the trajectory simulation is finished, the partial separation efficiency for each size is then evaluated.

RESULTS AND DISCUSSION

Downloaded At: 09:08 25 January 2011

Figure 3 shows typical simulated results of fluid velocity profile under a uniform feed velocity of 9.55 m/s and a split ratio of 0.62. In such a condition, the pressure drop through the hydrocyclone is 0.1 MPa. From the top-view of the velocity profile on the x-y plane at $z = 0$, as shown in Fig. 3(a), the velocity vectors decrease continuously from the entrance due to the downward flow in the cylindrical section. Although the fluid velocities on the solid walls are preset as zero, the velocity profile in the inlet conduit is not symmetrical to the central-line. The velocity near the inner wall is higher. This fact may result in a strong impact on the hydrodynamic wall when the fluid flows into the cylindrical part and results in a higher velocity near the wall, as shown in Fig. 3(b). Figure 3(b) shows the velocity profile on the x-z plane at $y = 0$. Since the sudden contraction of the cross-sectional area, the fluid velocity becomes higher when the fluid flows into the vortex finder, especially in the central region. It can be seen that the highest velocity over 11 m/s occurs in the middle but slightly lower region of the inlet conduit, and the velocities ranged from 5 to 7 m/s occur at the impact locations of the cylindrical wall and at the entrance region of the overflow conduit. The fluid velocities are lower than 2 m/s in most regions and close to zero on the vertical central-line. A line (or an envelope) of zero vertical velocity (LZVV) can be found in Fig. 3(b) as a V-character shape. According to the equilibrium orbit theory (13), the fluid flows upward inner the LZVV while flows downward outer the LZVV. These flows then constitute the overflow and underflow, respectively. In addition, re-circulating flows and small secondary eddies exist in the region around the cylindrical section, which may cause a short-circuit of particles flowing out through the vortex finder and then to worse efficiency and sharpness of particle separation. On the other hand, the fluid flows downward near

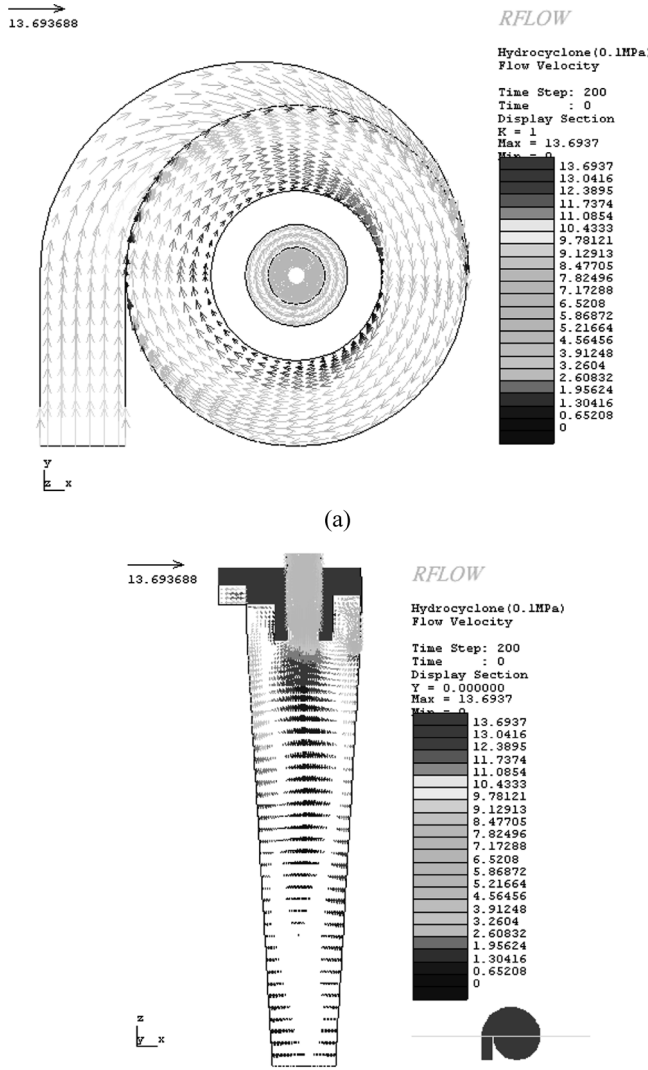

Figure 3. The simulated fluid velocity profiles under a uniform feed velocity of 9.55 m/s and a split ratio of 0.62, (a) top-view (on the x-y plane at $z = 0$), and (b) side-view (on the x-z plane at $y = 0$).

the hydrocyclone wall, but a part of it may change its flowing direction due to the conical shape of hydrocyclone and becomes the inner helical up-flow (secondary vortex).

Downloaded At: 09:08 25 January 2011

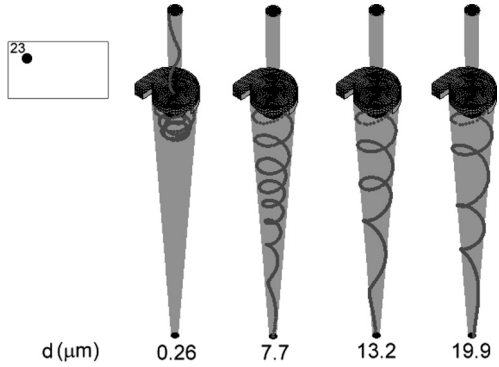

Figure 4. Simulated trajectories of $CaCO_3$-17 particles with different diameters initially at a specified inlet position under an inlet velocity of 7.55 m/s and a split ratio of 0.62.

Downloaded At: 09:08 25 January 2011

The particle trajectory in the hydrocyclone can be simulated using *RFLOW* software once the fluid velocity profiles are obtained. The typical results of $CaCO_3$-17 particles with different diameters under an inlet fluid velocity of 7.55 m/s and a split ratio of 0.62 are shown in Fig. 4. The initial positions of those particles are the same and marked as No. 23 on the inlet cross-section plane. For the smallest particle, $d = 0.26\,\mu m$, the particle finally migrates into the vortex finder after a few rotations. When the diameter is greater than 7.7 μm, particles are carried by the fluid flowing outside the LZVV and collected into the underflow after several rotations. It can be found that the rotation number decreases with increasing the particle size. These are attributed to the higher centrifugal and inertial forces acting on coarser particles. Higher centrifugal and inertial forces cause particles to deviate the fluid streamlines more easily. Therefore, the partial separation efficiency is higher for larger particles.

Figure 5 shows the effect of the inlet position on the trajectory of $CaCO_3$-17 particles with a diameter of 7.7 μm under a uniform inlet velocity of 7.55 m/s and a split ratio of 0.62. Four inlet positions are set and indicated in the figure. From the results of the velocity simulation, e.g., Fig. 3, one knows that the fluid near the lower region of the inlet conduit has higher velocity. Therefore, the particles at the initial positions of No.73 and 78 have more opportunities to be collected into the underflow. The trajectories of these two cases are almost the same; however, the particles initially at position No.78 can quickly move away from the cylindrical part (or vortex finder). It is because the particle is closer to the inner wall of the inlet conduit at where the fluid has higher velocity. On the other hand, for the particles initially at positions No.23 and 28,

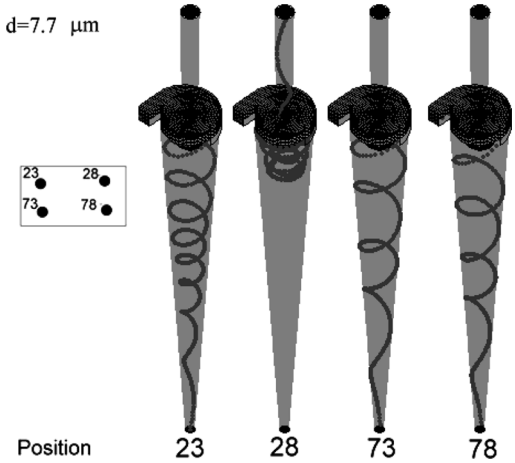

Figure 5. The effect of inlet position on the trajectory of $CaCO_3$-17 particles with a diameter of 7.7 μm under an inlet fluid velocity of 7.55 m/s and a split ratio of 0.62.

Downloaded At: 09:08 25 January 2011

their velocities are lower when they come into the cylindrical part. However, the particle initially at position No.23 is closer to the hydrocyclone wall, this means it has opportunities to collide on the hydrocyclone wall or to move into the primary vortex (the flowing stream outer the LZVV). Finally, it is collected into the underflow though it undergoes more rotations. It is expectable that the particle initially at position No.28 is able to flow into the vortex finder after a few rotations because of its low velocity and its location apart from the hydrocyclone wall. When the trajectory simulation is finished, the collection fraction or the partial separation efficiency of the particles can be calculated by summing the results of all 100 different inlet positions up.

In order to check the accuracy and practicability of *RFLOW* software, hydrocyclone experiments were carried out for comparison. $CaCO_3$-17 particles in JIS standard were dispersed in de-ionized water to prepare a 0.18 vol% suspension. The suspension was then separated by a 10-mm hydrocyclone manufactured by the Japan Chemical Engineering & Machinery Co. in Osaka, Japan. The detail structure is the same as that shown in Fig. 1. A comparison of partial separation efficiency between simulated results and experimental data is shown in Fig. 6. The temperature was kept at 20°C during the experiments. The inlet velocity and the split ratio were set as 9.55 m/s and 0.62, respectively. These resulted in a pressure drop of 0.1 MPa through the hydrocyclone. The partial separation efficiency for a given size of particles

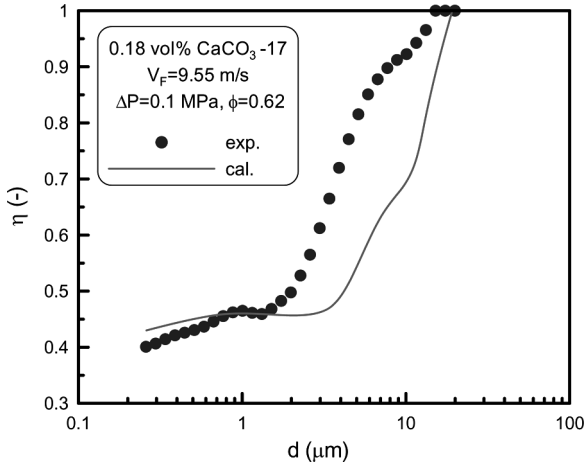

Figure 6. A comparison of partial separation efficiency of $CaCO_3$-17 particles between simulated results and experimental data.

Downloaded At: 09:08 25 January 2011

is defined as (14):

$$\eta(d) \equiv \frac{mass\,flow\,rate\,of\,particles\,with\,diameter\,d\,collected\,into\,under\,flow}{mass\,flow\,rate\,of\,particles\,with\,diameter\,d\,in\,the\,feed} \tag{3}$$

Its physical meaning can be considered as the collected fraction (or so-called "recovery") of particles with a diameter of d. As one can expect, an increase in the particle size leads to a higher separation efficiency. However, the separation efficiency keeps as high as 0.4 for submicron particles and does not drop to be zero for the smallest particles. This "fish-hook" phenomenon is attributed to the underflow and particle diffusion effects (12,14). A portion of fine particles are carried by the underflow liquid and collected together with those that are coarser. It can be seen that a larger deviation between simulated results and experimental data occurs for 5 to 10 μm particles. It is possible due to the neglect of the effects of particle shape or particle interactions, or due to the use of a symmetrical swirly turbulence model in simulations. However, the tendency is qualitative in agreement, and the predictions of d_{100} (the smallest diameter reaching 100% collection) and the fish-hook phenomenon are fairly well. The deviation of cut-size d_{50} (the diameter for 50% collection) between the simulated results and the experimental data is only 2 μm. Therefore, this simulation method is reasonably

Table 1. The calculated values of Q_o, Q_u, and ϕ for different overflow diameters under $V_F = 12.92\,\mathrm{m/s}$

D_o (mm)	2.0	3.0	4.0	5.0
Q_o (m^3/s)	2.51	3.22	3.56	3.74
Q_u (m^3/s)	2.71	2.01	1.65	1.47
ϕ	1.08	0.62	0.46	0.39

adopted to study the separation performances of hydrocyclones with different geometric structures in this study.

The influence of the overflow conduit diameter on the partial separation efficiency is studied numerically using *RFLOW* software. The same operation capacity, e.g. $V_F = 12.917\,\mathrm{m/s}$, is selected as the comparison basis. The other geometric structure parameters of hydrocyclone are all the same as their originals in simulations except the value of D_o. Since two outlet boundary conditions are both set as the atmospheric pressures, the flow rates at the overflow and underflow conduits will vary with the overflow diameter. The data of volumetric flow rates and split ratio under various overflow diameters are calculated as soon as the simulations are converged and listed in Table 1. It can be found that an increase in the overflow diameter leads to an increase in the fluid flow rate in the overflow. This results in a lower flow rate in the underflow and, consequently, a smaller split ratio. If the value of D_o increases 2-fold from 2 to 4 mm, the volumetric flow rate in overflow will be increased as high as 40%. Figure 7 depicts the variation of the partial separation efficiency with overflow diameter. When the overflow rate is increased by increasing the overflow diameter, particles have more opportunities to migrate into the vortex finder. The centrifugal force exerted on the particles in the primary vortex is also reduced due to the slower underflow. As a result, the separation efficiency decreases. According to the analysis on the separation mechanism of hydrocyclone in the previous study by the authors (12), the underflow effect is more significant for finer particles. This fact can be demonstrated by the results shown in Fig. 7. In addition, the separation efficiency of larger particles is primarily affected by the centrifugal effect (12); the influence of the overflow conduit diameter becomes less as the particle size increases, as shown in Fig. 7. The cut-diameter d_{100} is almost invariant with the size of overflow conduit.

Figure 8 shows the effect of underflow diameter on the partial separation efficiency under the same conditions as Fig. 7. The geometric structure parameters are all the same as their original indicated in Fig. 1 except the value of D_u. Since the shape of the conical part cannot be

Downloaded At: 09:08 25 January 2011

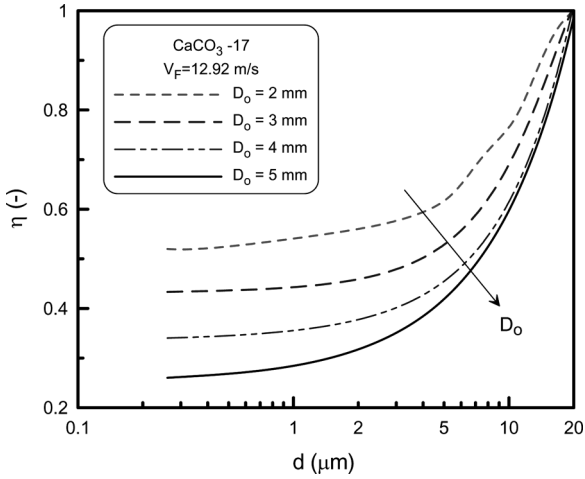

Figure 7. Effect of overflow diameter on the partial separation efficiency of particles.

Downloaded At: 09:08 25 January 2011

changed too much, the underflow diameter varies only from 1.4–2.2 mm. The flow rates and split ratio under various simulation conditions are calculated and listed in Table 2. The underflow rate and the split ratio increase markedly as the conduit diameter increases. Therefore, the

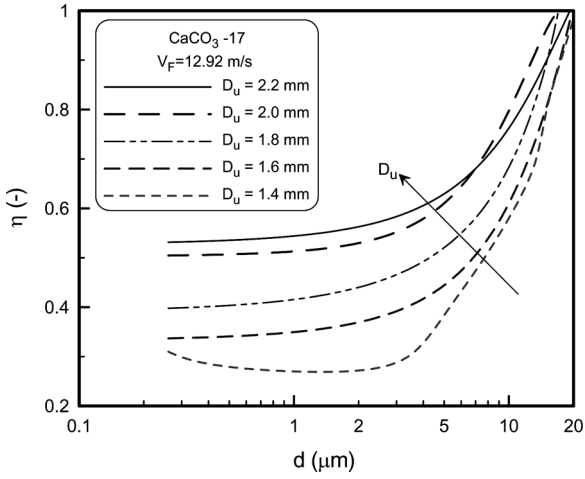

Figure 8. Effect of overflow diameter on the partial separation efficiency of particles.

Table 2. The calculated values of Q_o, Q_u and ϕ for different underflow diameters under $V_F = 12.92\,\mathrm{m/s}$

D_u (mm)	1.4	1.6	1.8	2.0	2.2
Q_o (m^3/s)	3.83	3.56	3.30	3.03	2.78
Q_u (m^3/s)	1.38	1.65	1.92	2.18	2.41
ϕ	0.36	0.46	0.58	0.72	0.87

Downloaded At: 09:08 25 January 2011

separation efficiency will be improved by increasing, even a little, the underflow diameter. The same as the discussions on Fig. 7, the underflow effect is more significant for finer particles. The partial separation efficiency for submicron particles is enhanced 2-fold when D_u increases from 1.4 to 2.2 mm. However, the fish-hook phenomenon will be more obvious for a small underflow diameter, e.g., $D_u = 1.4$ mm. The particles with a diameter of 2 μm behave with the minimum efficiency. The smaller submicron particles on the contrary perform at a higher separation efficiency. This is because the diffusion phenomenon is more significant for finer particles or under lower underflow rate. Furthermore, it can be found that increasing the underflow diameter markedly decreases the cut-diameter d_{50} and d_{100}; the hydrocyclone performance can be effectively improved through this modification. However, this advantage cannot be seen as D_u exceeds 2.0 mm. This is possible due to a little change in the cone angle. In addition, the increase in the diameter of overflow or underflow conduit leads to higher separation efficiency for small particles; it is unfavorable to the sharpness of particle separation. Comparing the results shown in Figs. 7 and 8, the effect of the underflow diameter is more significant on the particle separation than that of overflow.

In order to study more effects of structure parameters on the separation efficiency, several typical structures of hydrocyclone are constructed as shown in Fig. 9. The specifications of Case 1 are the same as those indicated in Fig. 1(a), which is manufactured by Japan Chemical Engineering & Machinery Co. in Osaka, Japan. The cross-sections of the entrance for all cases are in a rectangular shape. In Case 1, the inlet conduit has a width of 2.5 mm and a height of 1.6 mm. Both Cases 2 and 3 have similar geometric structures as Case 1. However, Case 2 has a 20° downward inclined inlet conduit, while Case 3 changes the aspect ratio of the inlet cross-section from 2.5:1.6 to 1.6:2.5. Cases 4 and 5 are established according to the specifications of Rietema and Bradley types. The geometric parameters of these hydrocyclones are summarized in Table 3. Comparing these different structures, the Rietema and the Bradley types have shorter conical parts and a larger cone angle. The diameters of the

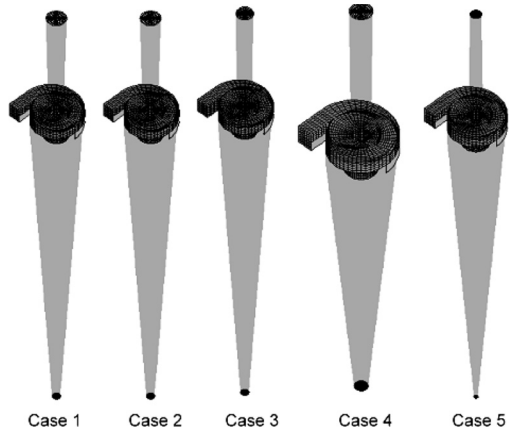

Figure 9. The geometric structures of five hydrocyclones used in simulation.

Downloaded At: 09:08 25 January 2011

underflow and the overflow conduits are particularly small for Bradley's hydrocyclone.

In this study, the effect of the particle inlet position on the separation efficiency is discussed by dividing the inlet cross-section into 10×10 grids. When the fluid velocity profile has been simulated, the particles with a given size distribution are released one by one from their initial positions and simulated their trajectories in the hydrocyclone by *RFLOW* software. The separation efficiency (collected fraction into the underflow) can then be evaluated. Figure 10 shows the simulated results of the separation efficiency at different initial inlet positions for three inlet installations, Cases 1–3. This comparison is based on the same operation capacity. Since the cross-sectional areas are the same for these cases, the inlet velocities are all set as 12.917 m/s and uniform profiles. The outlet boundary conditions are all set to be atmospheric pressures. The split

Table 3. The geometric structure parameters of test hydrocyclones

	D_i/D	D_o/D	D_u/D	I/D	L/D	θ
Case 1	0.16	0.34	0.16	0.42	7.7	6.0
Case 2	0.16	0.34	0.16	0.42	7.7	6.0
Case 3	0.16	0.34	0.16	0.42	7.7	6.0
Case 4	0.16	0.34	0.20	0.40	5.0	11.0
Case 5	0.16	0.20	0.07	0.33	6.85	8.5

0.25	1	1	0.5	0.5	0.25	0.11	0.11	0.25	0.25
1	1	0.75	0.11	0.11	0.25	1	1	1	1
0.25	0.25	0.75	0.75	0.25	0.11	0.11	0.11	0.11	0.75
0.11	0.25	0.5	0.25	0.25	0.11	0.25	0.5	0.25	0.5
0.25	0.5	0.75	1	0.75	1	0.11	0.25	0.75	0.5
0.5	0.75	0.75	0.5	0.5	0.5	0.5	0.25	0.25	1
0.75	0.75	1	0.75	1	1	1	0.75	0.75	1
0.5	1	1	1	0.75	1	1	1	0.5	1
0.25	1	1	1	1	1	1	1	1	1
0.5	0.75	0.25	0.5	1	1	1	0.75	1	0.5

(a) Case 1

0.25	1	1	1	1	1	1	1	1	0.25
0.5	0.25	0.75	0.75	0.5	0.5	0.5	0.75	1	1
0.25	0.75	0.5	0.5	0.5	0.5	0.25	0.11	0.25	1
0.25	1	1	0.75	0.25	0.11	0.25	0.25	0.5	1
0.5	0.5	0.5	0.25	0.25	0.25	0.25	0.25	0.25	1
0.11	0.25	0.25	0.25	0.25	0.5	0.25	0.25	0.5	1
0.25	0.11	0.25	0.75	0.25	1	1	1	1	1
0.25	0.75	0.75	0.5	0.75	0.75	0.75	1	1	1
0.25	1	1	1	1	1	1	0.5	0.75	1
0.5	0.75	1	0.5	0.5	0.5	0.5	0.25	0.25	0.75

(b) Case 2

0.75	0.5	0.11	0.25	0.11	0.5	0.11	0.25	0.25	0.11
0.11	0.5	0.5	0.25	0.11	0.11	0.5	0.25	0.5	0.25
0.5	0.25	0.5	0.5	0.11	0.25	0.25	0.5	1	0.5
0.25	0.5	0.25	0.25	0.25	0.25	0.5	0.75	0.75	1
0.5	0.25	0.25	0.5	0.11	0.25	0.5	0.75	0.75	1
0.75	0.75	0.75	0.11	0.5	0.75	1	1	1	1
0.5	0.25	0.25	0.75	0.75	1	1	1	1	0.11
0.11	0.25	1	1	1	1	1	1	1	0.25
0.25	0.75	1	1	0.75	0.25	0.75	1	1	0.75
0.25	0.5	1	0.25	0.25	0.25	0.5	1	0.25	0.11

(c) Case 3

Figure 10. Effect of inlet position on the separation efficiency for $CaCO_3$-17 particles under a uniform inlet velocity of 12.917 m/s in the hydrocyclones of (a) Case 1, (b) Case 2, and (c) Case 3.

Downloaded At: 09:08 25 January 2011

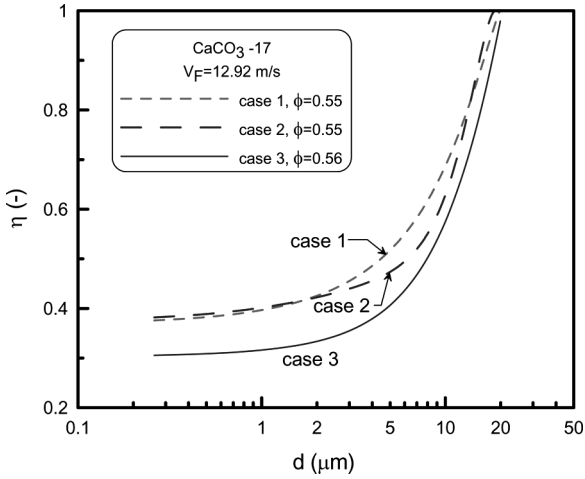

Figure 11. Comparison of partial separation efficiency among hydrocyclones of Cases 1, 2 and 3.

Downloaded At: 09:08 25 January 2011

ratios for these cases have a little difference even under the same operating conditions and are shown in Fig. 11. Comparing the results shown in Figs. 10(a) and (b), the higher efficiency occurs in the lower-half region for Case 1, while it occurs in the right-bottom region and near the right and top solid walls for Case 2. This is due to the different fluid velocity profiles in the inlet conduits of these cases. In general, the separation efficiency is more uniform distributed on the entrance plane for Case 2. When the inlet aspect ratio changes to 1.6:2.5, the higher efficiency distributes in the right-bottom region of the entrance plane for Case 3, as shown in Fig. 10(c). Comparing the overall efficiency of Cases 2 and 3 to Case 1, an inclined inlet conduit cannot improve the overall performance, on the contrary, which results in a 4% drop in the overall separation efficiency. A short-and-wide inlet is more efficient than a tall-and-narrow one. The overall efficiency of Case 3 decreases 15% lower than that of Case 1 although the inlet cross-sectional area and the mean fluid velocity are both the same.

The partial separation efficiencies of Cases 1–3 under the same condition as Fig. 10 are shown in Fig. 11. Comparing the curves of Cases 1 and 2, an inclined inlet conduit, Case 2, results in a 2 μm reduction in d_{100} but in a 3 μm increase in d_{50}. The partial separation efficiency of Case 2 is obviously lower for 2–10 μm particles. Indeed, the installation of an inclined inlet conduit has inessential effects on the separation efficiency of submicron particles. It can be also seen that the performance of

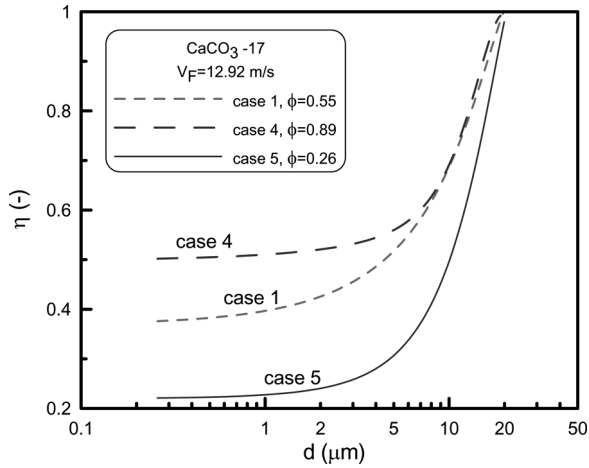

Figure 12. Comparison of partial separation efficiency among hydrocyclones of Cases 1, 4 and 5.

Downloaded At: 09:08 25 January 2011

Case 3 is worse due to a larger cut-size and lower partial separation efficiency than the other two cases. In conclusion, a short-and-wide inlet is more efficient for hydrocyclone design on the viewpoints of both partial and overall particle separation efficiency.

Figure 12 shows a comparison of partial separation efficiency among Cases 1, 4, and 5. The boundary conditions are set as the same as those in Figs. 10 and 11. However, the values of the split ratio for these cases have great discrepancies due to their different geometric structures. Case 4 has a particularly large split ratio due to a larger underflow diameter and shorter conical part, which leads more particles to be carried by quicker underflow. Therefore, the separation efficiency for the particles smaller than 7 μm is improved. However, the centrifugal effect cannot be enhanced effectively due to its large cone angle; the separation efficiency for those particles larger than 8 μm is almost the same as in Case 1. On the other hand, the split ratio of Case 5 is only a half of Case 1 because of an extreme small underflow diameter. This makes its efficiency markedly reduced especially for small particles. In fact, the values of d_{100} for these three cases are almost the same. This is because the comparison is based on the same hydrocyclone diameter and inlet velocity. However, the values of d_{50} in these cases are quite different, the sequence is Case 5 > Case 1 > Case 4. Comparing the partition curves shown in Fig. 12, Case 1 exhibits a higher separation sharpness than Case 4 and a higher separation efficiency than Case 5.

CONCLUSIONS

Computational fluid dynamics has been employed to study the effects of geometric structure parameters of 10 mm-diameter hydrocyclones on the particle separation efficiency. The particle trajectories and the partial separation efficiency were calculated once the fluid velocity profiles were simulated using *RFLOW* software with a standard isotropic k-ε turbulent model. The simulated partition curve exhibited a 20% deviation for 5–10 μm particles. However, the simulated d_{50} was only 2 μm larger than that measured in experiments, while the value of d_{100} could be accurately simulated. The separation efficiency could be improved by enlarging the underflow conduit or reducing the overflow diameter; however, the separation sharpness became less clear through these modifications. For the rectangular inlets, a short-and-wide rectangular inlet was more efficient for particle separation than a tall-and-narrow one. An inclined inlet conduit played an inessential role on the efficiency improvement. Comparing typical hydrocyclones with the same size, the hydrocyclone used in the experiments of this study had a higher separation sharpness than the Rietema type and a higher efficiency than the Bradley type based on the same operation capacity.

Downloaded At: 09:08 25 January 2011

ACKNOWLEDGEMENTS

The authors wish to express their sincere gratitude to the National Science Council (NSC), R.O.C. for the financial supports. The supply of hydrocyclone system and particulate samples for experiments by the Japan Chemical Engineering & Machinery Co. in Osaka, Japan, and the providing of *RFLOW* software by RFLOW Co. Ltd in Tokyo, Japan, are also highly appreciated.

NOTATIONS

C_L	length of the cylindrical part of hydrocyclone (m)
d	particle diameter (m)
d_{50}	the particle diameter for 50% separation efficiency (m)
d_{100}	the smallest particle diameter for 100% separation efficiency (m)
D	diameter of hydrocyclone (m)
D_i	diameter of the inlet conduit (m)
D_o	diameter of the overflow conduit (m)
D_u	diameter of the underflow conduit (m)
g	gravitational acceleration (m/s^2)
I	length of the straight part of inlet conduit (m)
L	length of the conical part of hydrocyclone (m)

p hydraulic pressure (Pa)
ΔP pressure drop through hydrocyclone (Pa)
Q_o volumetric flow rate of overflow(m^3/s)
Q_u volumetric flow rate of underflow(m^3/s)
t time (s)
v velocity vector (m/s)
V_F mean fluid velocity at the inlet (m/s)

Greek Letters

ρ density of liquid (kg/m^3)
μ liquid viscosity (Pa s)
μ_e eddy viscosity (Pa s)
ϕ split ratio of underflow to overflow rate (−)
η partial separation efficiency (−)
θ cone angle of hydrocyclone (degree)

Downloaded At: 09:08 25 January 2011

REFERENCES

1. He, P.; Salcudean, M.; Gartshore, I.S. (1999) A numerical simulation of hydrocyclones. *Trans IChemE.*, *77*: 429.
2. Cullivan, J.C.; Williams, R.A.; Cross, C.R. (2003) Understanding the hydrocyclone separator through computational fluid dynamics. *Trans IChemE. Part A.*, *81*: 455.
3. Cullivan, J.C.; Williams, R.A.; Dyakowski, T.; Cross, C.R. (2004) New understanding of a hydrocyclone flow field and separation mechanism from computational fluid dynamics. *Miner. Eng.*, *17*: 651.
4. Schuetz, S.; Mayer, G.; Bierdel, M.; Piesche, M. (2004) Investigations on the flow and separation behaviour of hydrocyclones using computational fluid dynamics. *Int. J. Miner. Process.*, *73*: 229.
5. Grady, S.A.; Wesson, G.D.; Abdullah, M.; Kalu, E.E. (2003) Prediction of 10-mm hydrocyclone separation efficiency using computational fluid dynamics. *Filtr. Sep.*, *11*: 41.
6. Olson, T.J.; Van Ommen, R. (2004) Optimizing hydrocyclone design using advanced CFD model. *Miner. Eng.*, *17*: 713.
7. Narasimha, M.; Sripriya, R.; Banerjee, P.K. (2005) CFD modeling of hydrocyclone – prediction of cut size. *Int. J. Miner. Process.*, *75*: 53.
8. Wang, B.; Yu, A.B. (2006) Numerical study of particle-fluid flow in hydrocyclones with different body dimensions. *Miner. Eng.*, *19*: 1022.
9. Bhaskar, K.U.; Murthy, Y.R.; Raju, M.R.; Tiwari, S.; Srivastava, J.K.; Ramakrishnan, N. (2007) CFD simulation and experimental validation studies on hydrocyclone. *Miner. Eng.*, *20*: 60.
10. Pasquier, S.; Cilliers, J.J. (2000) Sub-micron particle dewatering using hydrocyclones. *Chem. Eng. J.*, *80*: 283.

11. Cilliers, J.J.; Diaz-Anadon, L.; Wee, F.S. (2004) Temperature, classification and dewatering in 10 mm hydrocyclones. *Miner. Eng.*, *17*: 591.
12. Hwang, K.J.; Hsueh, W.S.; Nagase, Y. (2008) Mechanism of particle separation in small hydrocyclone. *Drying Technol.*, 26: 1002.
13. Kawatra, S.K.; Bakshi, A.K.; Rusesky, M.T. (1996) Effect of viscosity on the cut (d_{50}) size of hydrocyclone classifiers. *Miner. Eng.*, *9*: 881.
14. Frachon, M.; Cilliers, J.J. (1999) A general model for hydrocyclone partition curves. *Chem. Eng. J.*, *73*: 53.

Downloaded At: 09:08 25 January 2011